RSC Pharmaceutics

ROYAL SOCIETY OF CHEMISTRY

PAPER

View Article Online
View Journal | View Issue

Cite this: *RSC Pharm.*, 2025, **2**, 749

Tailoring bromelain-loaded lipid–polymer hybrid nanoparticles for asthma management: fabrication and preclinical evaluation†

Manu Sharma * and Namita Gupta

Poor response and associated side effects of available drugs in clinics have limited successful asthma management. Traditionally, bromelain has been found effective in asthma management; however, its use is limited by the need for high oral doses and poor bioavailability. Therefore, the present investigation was tailored to prepare bromelain-loaded lipid–polymer hybrid nanoparticles (Br-LPHNs) to enhance the oral bioavailability and therapeutic efficacy of bromelain in the management of allergic asthma. Br-LPHNs, consisting of a lipid core encapsulated in a biomimetic polymethylmethacrylate coating, were prepared utilizing the double emulsion solvent evaporation method. The drug release behavior, mucolytic potential and stability of the optimized formulation were evaluated. Pharmacokinetic and pharmacodynamic studies were executed in an allergen-induced asthma model. The optimized Br-LPHNs exhibited a nano-size (190.91 ± 29.48 nm) and high entrapment efficiency (89.94 ± 3.98%), along with gastro-resistant and sustained drug release behavior for up to 24 h. Using LPHNs as a carrier improved shelf life (~6.99-fold) and bioavailability (6.89-fold) compared to pure bromelain. The optimized formulation significantly suppressed bronchial hyperresponsiveness, delayed the onset of bronchospasm and reduced its severity. Moreover, oxidative and immunological markers were significantly ($p < 0.05$) reduced, accompanied by the restoration of antioxidant enzyme levels to normal. Histopathological investigations also confirmed reduced tissue injury. Thus, the development of Br-LPHNs not only ensured *in vitro* and *in vivo* stability of bromelain but also offered a promising approach for asthma management.

Received 8th December 2024,
Accepted 18th April 2025

DOI: 10.1039/d4pm00327f

rsc.li/RSCPharma

Introduction

Asthma is a complicated and multifactorial chronic inflammatory respiratory disease with a complex pattern of inheritance.[1,2] It is characterized by multicellular inflammation, bronchospasm, airway obstruction and airway hyperresponsiveness, accompanied by episodes of wheezing and spasmodic coughing often worsening at night. Asthma is typically triggered by both specific and broad environmental stimuli.[3] The majority of the reversible or permanent pathophysiological alterations in the airway wall during asthma are caused by the acute activation and accumulation of inflammatory cells, increased expression of helper T cells, dysplasia of goblet cells and airway muscles and changes in the quantity and quality of mucus production.[4] This cascade of molecular events generates an oxidative environment that impairs the lung's antioxidant defenses and promotes the destruction of macromolecules.[5]

Current medications, such as inhaled β-agonists and glucocorticoids, are among the most effective therapies for asthma management. These treatments can reduce airway inflammation, alleviate bronchoconstriction and improve quality of life for many patients; however, they fail to address the structural abnormalities induced by the disease. In addition, long-term use may lead to serious side effects, such as high blood pressure, cataracts, osteoporosis in older adults and slowed growth in children.[6,7] Furthermore, a sizable portion of patients do not respond adequately to these medications, resulting in inadequate asthma management.[8] Therefore, there is a crucial need to explore novel alternative therapies for asthma in clinical settings. Scientists and pharmaceutical researchers are increasingly focusing on herbal therapies for asthma management, driven by encouraging results from clinical and experimental studies.[9,10]

In traditional systems of medicine, bromelain exhibits potential pleiotropic therapeutic benefits, functioning as a mucolytic,[11] wound-healing,[12] fibrinolytic,[13] antithrombotic,[14] anti-inflammatory,[15] antioxidant,[16] anticancer[17] and immuno-

Department of Pharmacy, Banasthali Vidyapith, Rajasthan, 304022, India.
E-mail: aasmanu2018@gmail.com, sharmamanu10@gmail.com;
Tel: +91-9001701324

† Electronic supplementary information (ESI) available. See DOI: https://doi.org/10.1039/d4pm00327f

modulatory agent.[18] Previous studies have shown that bromelain effectively reduces airway reactivity and irritant susceptibility in ovalbumin-induced allergic airway disease by decreasing levels of lung inflammation markers.[19,20] Bromelain also inhibits the expression of cyclooxygenase-2 and prostaglandin E2, while reducing cytokine production activated during inflammatory conditions.[21,22] The downregulation of inflammation is further supported by bromelain's proteolytic breakdown of cell surface signals, which facilitates the homing and migration of lymphocytes to the site of inflammation.[23] Furthermore, bromelain regulates the expression of transforming growth factor (TGF)-β, a key regulator of inflammation.[24] However, the high dose, poor shelf life and mechanical and gastric instability limit its therapeutic potential. The vulnerability of bromelain to degradation, denaturation or agglomeration in the gastric environment may lead to unpredictable hypersensitivity reactions or toxic effects, along with a loss of therapeutic efficacy.[15,25] This highlights the need for exploring novel formulation strategies to develop a stable and patient-compliant oral bromelain therapy for asthma management.

Nano-scale carriers in the field of nanomedicines have gained significant attention in the development of novel formulations for proteins and peptides. Polymeric nanoparticles, solid lipid nanoparticles and liposomes have emerged as prominent nanocarriers to enhance absorption across the GIT *via* distinct absorption mechanisms.[26–28] However, encapsulating bromelain, a hydrophilic molecule, in polymer or lipid-based nanocarriers is notably challenging due to its rapid partitioning into the aqueous phase during formulation development. Liposomes, on the other hand, have enormous potential for encapsulating hydrophilic drugs. However, their inconsistent and uncertain absorption, coupled with their inability to maintain structural integrity at the absorption site, limits their oral delivery.[28] To overcome the limitations of prevailing systems, lipid–polymer hybrid nanoparticles (LPHNs) have been proposed as a robust design, featuring a lipid core enveloped in a polymeric layer. The lipid core prevents the partitioning of hydrophilic drugs by forming a molecular barrier to the aqueous environment, while the polymeric layer ensures structural integrity and provides a biomimetic shield. Numerous reports in the literature confirm the successful fabrication of LPHNs for hydrophilic drugs, despite the use of polymeric nanocarriers.[29,30] The use of polymethylmethacrylate (PMMA), a pH-sensitive polymer, additionally protects proteins and enzymes from the acidic environment of the stomach while mimicking drug release in the intestine.[31] Furthermore, the core–shell architecture of LPHNs restrict the inward permeation of gastrointestinal fluids, facilitating prolonged drug release. The distinctive characteristics of LPHNs, such as their nanosize that facilitates rapid stomach emptying, increased surface area, site-specific controlled delivery, enhanced cellular absorption, reduced first-pass metabolism and associated adverse or toxic effects, enhanced bioavailability and improved patient compliance, have increased their acceptance for delivering challenging molecules like proteins.[29,30] To the best of our knowledge, no reports are available in the literature regarding the formulation of bromelain-loaded LPHNs (Br-LPHNs).

The present study was undertaken to develop and optimize Br-LPHNs using lecithin as the lipid and PMMA as the polymer. Furthermore, the optimized nanoparticulate formulation was analyzed for its release behavior, stability, pharmacokinetics and anti-asthmatic activity in guinea pigs as an animal model.

Experimental

Materials

Poly methyl (methacrylate) (Mol wt. 100.12 g mol^{-1}), bromelain, casein, tyrosine and trichloro acetate (98.0%) were obtained from Himedia laboratory Pvt. Ltd, Mumbai, India. Polyvinyl alcohol (PVA) and mannitol were purchased from S.D Fine Chemicals Ltd, Mumbai. Dichloromethane (DCM) was obtained from Merck, Germany. All other chemicals and solvents were of analytical grade and used without further purification. Double-distilled water was used throughout the study.

Fabrication of Br-LPHNs

Br-LPHNs were prepared using a double emulsion solvent evaporation technique with slight modifications.[14] Bromelain and soya lecithin were co-dissolved in Tris–HCl buffer (pH 5.0), which constituted the aqueous phase. The primary emulsion (w/o) was formed by the dropwise addition of the aqueous phase to the organic phase while being sonicated (20 W power, 20% amplitude) for 7 min at 4 °C. The organic phase consisted of PMMA dissolved in dichloromethane with a surfactant (0.5% w/w, Span 80). The primary colloidal dispersion was further emulsified by dropwise addition into aqueous PVA (1% w/v) under probe sonication at 4 °C. The resulting double emulsion was then agitated at room temperature (100 rpm, 12 h) to enable complete removal of the organic solvent. To remove free bromelain and unused surface-active agent, the nanoparticulate dispersion was centrifuged at 22 000 rpm for 15 min at 4 °C, followed by washing twice with distilled water. Finally, the recovered nanoparticle pellet was dispersed in a mannitol solution (10% w/v) and lyophilized. Ultimately, the pellet of recovered nanoparticles was dispersed in a cryoprotectant solution containing 10% w/v mannitol. Lyophilized formulations were stored in an airtight container at 4 °C for further examinations. Various process variables, such as lipid and polymer concentration, drug loading, volume of the continuous phase and sonication time, were optimized to achieve a formulation with a nanosize range, high entrapment efficiency and good colloidal properties (Table 1).

Characterization of Br-LPHNs

Particle size, polydispersity index (PDI) and zeta potential. The average particle size, PDI and zeta potential of the prepared Br-LPHNs were estimated using a Nano ZS (Malvern, Germany). Samples were dispersed in double-distilled water and appropriately diluted prior to estimation.

Table 1 Effect of different processing variables on quality parameters, such as size, PDI, zeta potential and entrapment efficiency

Formulation code	Polymer (mg)	Soya lecithin (mg)	Drug (mg)	Sonication time		Continuous phase volume (ml)	Particle size (nm ± SD)	PDI (PDI ± SD)	Zeta potential (mV ± SD)	Entrapment efficiency (%±SD)
				Pre time	Post time					
H_1	200	25	25	7	15	30	286.43 ± 38.61	0.18 ± 0.01	−10.46 ± 1.87	63.05 ± 2.31
H_2	200	50	25	7	15	30	230.56 ± 25.25	0.25 ± 0.01	−20.06 ± 1.90	72.13 ± 2.09
H_3	200	75	25	7	15	30	375.33 ± 42.61	0.39 ± 0.01	−8.36 ± 1.45	66.32 ± 2.23
H_4	200	50	30	7	15	30	190.91 ± 29.48	0.14 ± 0.02	−28.30 ± 2.08	89.94 ± 3.98
H_5	200	50	50	7	15	30	292.23 ± 30.50	0.18 ± 0.01	−14.16 ± 3.66	76.38 ± 2.51
H_6	200	50	30	7	15	40	314.83 ± 42.55	0.28 ± 0.02	−18.67 ± 1.11	78.64 ± 3.11
H_7	200	50	30	5	15	30	642.9 ± 68.25	0.67 ± 0.05	−15.78 ± 2.00	60.29 ± 5.29
H_8	200	50	30	9	15	30	328.83 ± 45.63	0.27 ± 0.01	−29.33 ± 1.20	66.12 ± 5.66
H_9	200	50	30	7	20	30	449.2 ± 36.39	0.32 ± 0.01	−31.73 ± 1.37	63.34 ± 7.63

Entrapment efficiency. Briefly, the clear supernatant collected after centrifugation at 22 000 rpm for 15 min at 4 °C from the nanoparticulate formulations before lyophilization was appropriately diluted for analysis of free bromelain content using the Lowry method. The analysis was conducted using a UV/Vis spectrophotometer (Labindia® UV 3000+, Mumbai, India) at 750 nm.[32] Entrapment efficiency (EE) was determined using the following formula:

$$\mathrm{EE}(\%) = \frac{\text{amount of bromelain added} - \text{amount of bromelain in supernatant}}{\text{amount of bromelain added}} \times 100 \quad \text{(i)}$$

Morphology. Field emission scanning electron microscopy was used to analyze the morphology of the lyophilized materials. The lyophilized samples were mounted on aluminum stubs using carbon adhesive tape and observed at a working distance of 30 mm and an acceleration voltage of 5 kV, with images subsequently captured.

Structural integrity. The conformational integrity of bromelain in the freeze-dried nanoparticles was analyzed qualitatively using a fluorescence spectrometer (Perkin–Elmer LS 45). A freeze-dried formulation equivalent to 1 mg of bromelain was dispersed in dichloromethane to lyse the vesicles and centrifuged at 22 000 rpm at 4 °C. The collected pellet was dissolved in distilled water and analyzed using the fluorescence spectrometer to acquire the emission spectrum (250–500 nm) of the samples at an excitation wavelength of 280 nm and a scan rate of 100 nm min^{-1}. The correction in each protein spectrum was made by subtracting the spectrum of the blank solution.[33]

Subsequently, pure drug and lyophilized optimized formulation were subjected to different pH environments, *i.e.*, pH 1.2 and 6.8, corresponding to the stomach and small intestine, respectively, to evaluate their stability in the gastrointestinal tract. In detail, precisely weighed pure drug and Br-LPHNs nanoparticles equivalent to 2 mg bromelain were dispersed in HCl buffer (pH 1.2) and phosphate buffer (pH 6.8), respectively, followed by incubation at 37 ± 0.5 °C with 100 shakes per minute for 2 h. The substantial effect of the respective conditions after incubation on the conformational integrity of bromelain was determined qualitatively using a fluorescence spectrometer.

Dissolution profile. *In vitro* bromelain release from Br-LPHNs was evaluated using the dialysis membrane method.[16] A dialysis sac containing Br-LPHNs (equivalent to 50 mg of bromelain) was immersed in pH-progressive dissolution media (100 ml), starting with HCl buffer (pH 1.2) for 2 h, followed by phosphate buffer (pH 6.8), and maintained at 37 ± 2 °C with continuous agitation at 100 rpm. Aliquots (2.5 ml) were withdrawn at regular time intervals up to 24 h, replenished with the same volume of the respective buffer after each withdrawal and analyzed spectrophotometrically at 750 nm for protein content.

Mucolytic activity. The artificial mucus, exhibiting viscoelastic behavior similar to human airway mucus, was prepared by slowly mixing locust bean gum (1% w/v) into preheated sodium nitrite solution (1% w/v) at 80 °C, followed by continuous stirring on a magnetic stirrer for 24 h. Volume losses due to evaporation were compensated by adding sufficient sodium nitrite solution as needed. The galactomannan chains in the locust bean gum solution were cross-linked by the addition of 0.1 M sodium tetraborate.[34] The resulting mucus (2 g) was incubated at 37 °C in an orbital shaker at 100 rpm with the drug (0.2% w/w) and Br-LPHNs dispersion (equivalent to 0.2% w/w bromelain). The comparative evaluation of the effect of the drug and Br-LPHNs dispersion on the viscoelastic properties of artificial mucus was determined at predetermined time intervals of 2, 4, 6, 8 and 24 h using a rheometer (Brookfield D 220, USA) at 25 °C.

Stability studies. Pure drug and lyophilized formulations were assessed for their stability according to ICH guidelines to determine their suitable storage conditions and shelf-life. Samples sealed in airtight amber-colored glass vials were stored under accelerated temperature conditions (40 ± 2 °C/75 ± 5% RH) and room temperature conditions (25 ± 2 °C/60 ± 5% RH) for 6 and 12 months, respectively. At specified time

intervals (0, 1.5, 3, 6, 9 and 12 months), samples were withdrawn and evaluated for the percentage of proteolytic activity of bromelain remaining.[15]

***In vivo* studies.** The current animal study was duly approved by the Banasthali Vidyapith IAEC (574/GO/ReBi/S/02/CPCSEA), in compliance with the guidelines of CPCSEA, Ministry of Social Justice and Empowerment, Government of India. Adult guinea pigs (300–450 g) and Wistar rats (220 ± 20 g) of either sex were used for the animal studies. The animals were housed with free access to pelleted food and water *ad libitum* under a 12 h light–dark cycle at 22 ± 1 °C and 55 ± 5% RH throughout the study.

Pharmacokinetic studies. Wistar rats were randomly assigned to two groups (n = 12). Group I animals received a drug solution (40 mg kg^{-1}), while group II was administered Br-LPHNs (equivalent to 40 mg kg^{-1} bromelain) by oral gavage. Blood samples (250 μl) were subsequently withdrawn from the rat tail vein at pre-dose (0.0), 0.5, 1, 2, 4, 6, 8, 12 and 24 h post-treatment. Plasma was collected by centrifuging the blood at 3000 rpm for 5 min at 4 °C and analyzed for bromelain's proteolytic activity, corresponding to the bromelain content.[14,15] Winnonin® 6.1 (Pharsight Corporation, Mountain View, CA) pharmacokinetic software was used to determine various pharmacokinetic parameters using non-compartmental analysis.

Pharmacodynamics studies. Intraperitoneal injections of OVA solution (150 μg ovalbumin and 100 mg aluminum hydroxide emulsified in 1 ml of normal saline) were administered to sensitize 20 healthy guinea pigs weighing 250–300 g on the first and seventh days, followed by a booster dose on day 14.[35] Subsequently, guinea pigs were randomly assigned equally into 4 groups (n = 6). Group I animals received normal saline, whereas groups II, III and IV were administered chlorpheniramine maleate (10 mg kg^{-1}), bromelain solution (10 mg kg^{-1}) and optimized Br-LPHNs (10 mg kg^{-1}, equivalent to bromelain) for 7 days. Similar to OVA-sensitized animals, six naïve animals were sham-sensitized with normal saline.

Following seven days of sequential treatment, animals in each group were challenged with a histamine dihydrochloride solution (1% w/v). The animals' physiological reactions, survival, pre-convulsive dyspnea (PDT) and recovery time (RT) were monitored during the study.[36] The following formula was used to calculate the percentage of protection provided against asphyxia:

$$\%\ \text{Protection} = \frac{\text{BT1}}{\text{BT2}} \times 100, \qquad \text{(ii)}$$

where BT1 denotes the time at which bronchospasm began in the control group, and BT2 denotes the time at which bronchospasm began following pretreatment with standard or test samples.

Following exposure to histamine aerosols, animals were sacrificed to obtain blood samples *via* heart puncture and to collect organs such as the trachea, liver, spleen and lungs. Hematological parameters such as WBC, hemoglobin level, blood cell counts, TNF-α, IL-5 and IgG were assessed. Additionally, oxidative stress markers such as lipid peroxidation (LPO), protein carbonyl content, myeloperoxidase (MPO) activity, reduced glutathione (GSH), superoxide dismutase (SOD), catalase and nitric oxide (NO) levels were estimated in tissue homogenates to assess their antigen-specific response.[14,27]

Bronchoalveolar fluid analysis. Immediately following blood collection, the trachea of sacrificed animals was carefully exposed and cannulated. Five bronchoalveolar lavages were performed by infusing normal saline through the cannula, followed by aspiration after gently massaging the lungs. The obtained samples were combined to calculate the total number of cells per milliliter using a Neubauer hemocytometer after staining with Giemsa stain.[35] Simultaneously, the separated BAL fluid was evaluated for eosinophil count, immunological markers (TNF-α, IL-5 and IgG) as well as oxidative stress markers.

Statistical analysis. Dunnett's *post hoc* test and one-way ANOVA were used for statistical analysis in GraphPad Prism version 5.00 (GraphPad Software, California, USA). The differences were considered statistically significant at $p < 0.05$ in all studies.

Results and discussion

Optimization of Br-LPHNs

Various process variables were optimized, considering mean particle size, entrapment efficiency, PDI and zeta potential as the framework. An increase in the soya lecithin-to-drug weight ratio from 1 : 1 to 2 : 1 positively influenced the entrapment efficiency and reduced the particle size due to the amphiphilic nature of soya lecithin. This might be attributed to the physical adsorption of soya lecithin at the interface of the primary emulsion (w/o), which hindered the permeation of the drug into the external aqueous phase (Table 1).[37] However, further increases in the lipid-to-drug ratio (3 : 1) reduced entrapment efficiency, with an increase in particle size and PDI, owing to its positive effect on matrix viscosity, which might have prevented effective particle size reduction (Table 1).[38] Simultaneously, a higher lipid amount also promoted the formation and assembly of lecithin vesicles. The coexistence of lecithin vesicles might contribute to the growth of particle size and the reduction of their zeta potential.[39] In addition, the relative increase in polymer load at a drug-to-polymer weight ratio of 1 : 6.67 improved entrapment efficiency by facilitating rapid film formation over the core material, which helped in stabilizing the nanoparticulate structure and delayed solvent and non-solvent counter-diffusion.[29,40] However, a further increase in polymer load at a drug-to-polymer weight ratio of 1 : 8 resulted in a lower real drug load, which in turn led to reduced entrapment efficiency. A higher polymer proportion also favored the formation of a coarse dispersion, as illustrated by a greater PDI, due to insufficient energy to overcome the viscous forces (Table 1).[16,27]

A higher external phase volume remarkably increased particle size and PDI, with a decrease in encapsulation efficiency

owing to the lack of ample shear forces for the development of uniform, stable micellar structures (Table 1).[27,29]

The sonication period during primary and double emulsion preparation had a substantial impact on particle size, entrapment efficiency and colloidal properties. An increase in sonication time accelerated the production of smaller particles with higher entrapment efficiency by creating consistent micellar structures during the primary (7 min) and secondary (15 min) emulsification steps. Nevertheless, further escalation of sonication duration during primary (9 min) and secondary emulsification (20 min) resulted in increased particle size and PDI, along with lower zeta potential and entrapment efficiency, respectively (Table 1). The disruption of the interfacial barrier during micellization, due to high shear forces, might have facilitated the coalescence of the dispersed phase.[15,16]

The H_4 formulation, exhibiting the highest entrapment efficiency (89.94 ± 3.98%) with homogeneously dispersed nanoparticles (190.91 ± 29.48 nm), was chosen for additional studies.

SEM analysis of the optimized batch revealed a uniform spherical shape with a size of approximately 200 nm (Fig. 1A).

Bromelain's integrity

The conformational integrity of bromelain encapsulated in nanoparticles was further evaluated by fluorescence spectroscopy. The emission spectrum of pure bromelain and bromelain released from the optimized formulation revealed a λ_{max} at 330 nm, corresponding to the intense emission of tryptophan. However, a slight decline in fluorescence intensity of bromelain leached from the optimized formulation was observed, without any shift in λ_{max} (Fig. 1B). The results confirmed that the formulation parameters were suitably optimized and maintained the conformational integrity of the tertiary structure of bromelain during encapsulation.[41]

In contrast, pure drug incubated at simulated gastric pH showed significantly lower fluorescence intensity, with a shift in λ_{max} to 343 nm. The red shift in λ_{max} for pure bromelain incubated in the gastric milieu pH might be attributed to conformational changes near the tryptophan surface, indicating denaturation of bromelain in the acidic environment.[42] However, no change in the aromatic chromophore of bromelain recovered after lysis of the nanoparticulate formulation,

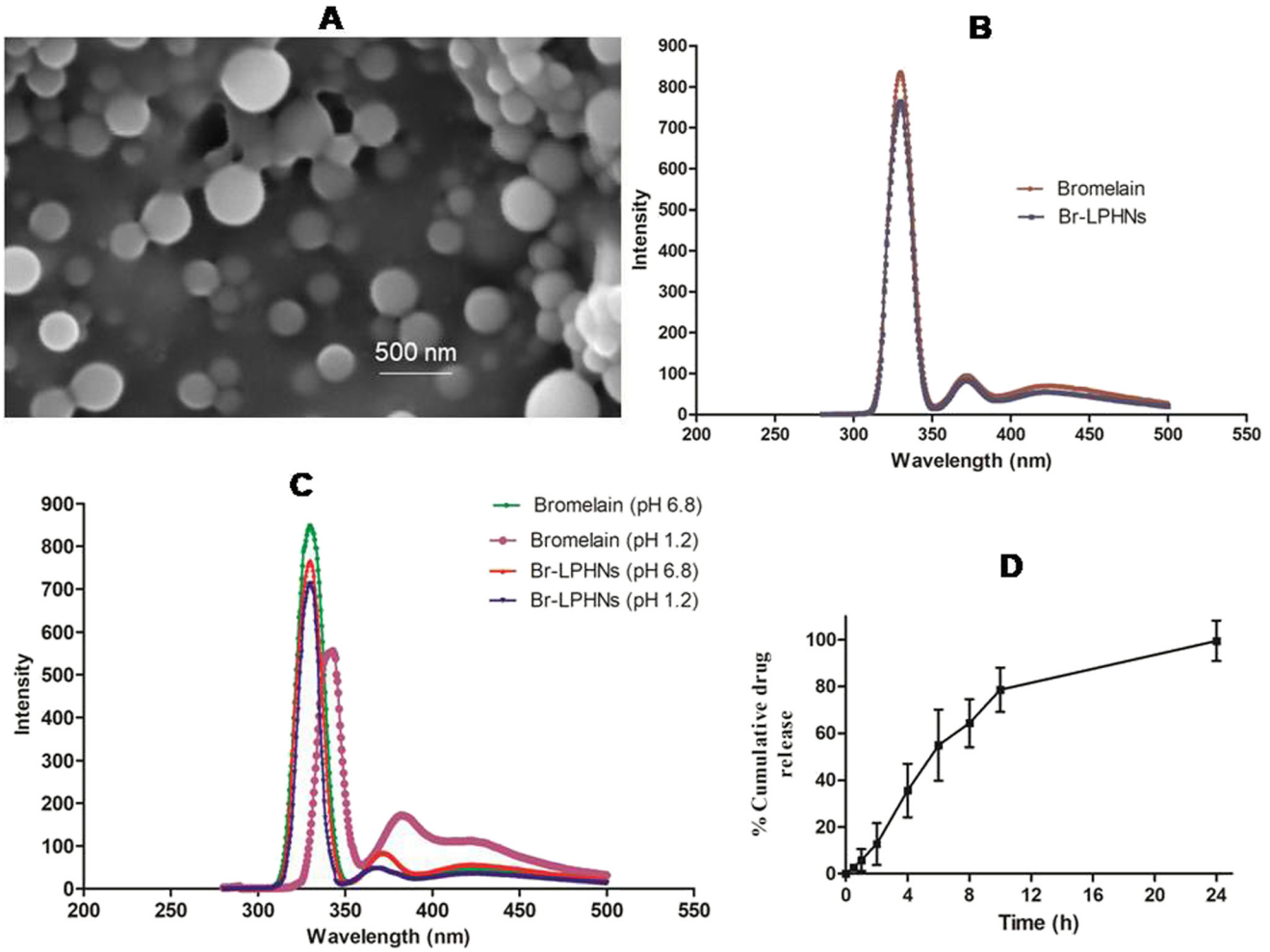

Fig. 1 (A) Scanning electron microscopy image of optimized formulation (H_4). (B) Fluorescence spectra of bromelain and bromelain released from Br-LPHNs respectively, (C) Fluorescence spectra of bromelain and Br-LPHNs incubated at simulated gastric pH 1.2 and simulated intestinal pH 6.8 respectively. (D) Dissolution profile of the H_4 formulation in pH-progressive dissolution media.

which had been incubated under simulated gastrointestinal pH, was observed (Fig. 1C). The results further confirmed that the structural protection offered by the vesicular system helped in maintenance of the tertiary structure as well as the proteolytic activity of bromelain in Br-LPHNs.[43]

Drug release

A dissolution study was conducted in pH-progressive media to evaluate the potential of Br-LPHNs in modulating drug release and extending bromelain's action. The optimized formulation at simulated gastric pH showed ~11% drug release in 2 h. The desorption of surface-adsorbed or weakly bound drug, or partial film flaws developed during lyophilization, might contributed to the initial drug release when the polymer coat remained unionized. Subsequently, a rapid increase in drug release over 2 h, followed by a prolonged release up to 24 h, was observed as the pH of the dissolution media was raised to pH 6.8 to mimic the pH of the small intestine (Fig. 1D). The sustained release may be attributed to the hindrance provided by the lecithin and PMMA envelope, which limited the inflow of the dissolution medium and the diffusion of bromelain from the core.[29,38] Furthermore, the dissolution data of Br-LPHNs were fitted to different release kinetic models to ascertain the drug release mechanism. The Korsmeyer–Peppas model was the best fit release model for the optimized formulation, as indicated by the highest R^2 value (0.978). The release exponent's numerical value (n = 0.73) demonstrated that a combination of diffusion and dissolving phenomena governed bromelain release.

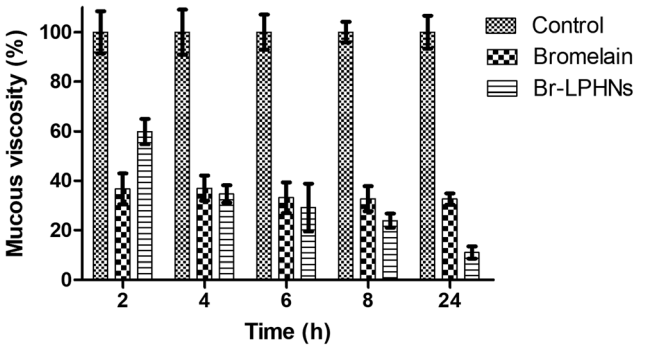

Fig. 2 Effect of pure drug solution and Br-LPHNs, at an equivalent amount of 0.2% w/w bromelain, on the viscosity of artificial mucus at varying time intervals respectively.

Mucolytic activity

Secretory epithelial cells typically secrete gel-forming polymeric mucins, the principal component of mucus. Thus, artificial mucus composed of cross-linked locust bean gum mucilage was used to mimic the viscoelastic behavior of real human airway mucus.[44] Upon exposure of artificial mucus to pure bromelain, a remarkable decrease in mucous viscosity was observed due to the disruption of glycosidic bonds and the splitting of proteins into smaller fragments.[45,46] The optimized formulation initially exhibited a lower degree of mucus

Table 2 Effect of storage conditions on the percentage bromelain content in the pure drug and Br-LPHNs

		Bromelain activity remaining (% ± SD)*							
Storage condition	Sample	0 M	1.5 M	3 M	6 M	9 M	12 M	K_{calc} (days^{-1})	t_{90} (days)
25 ± 2 °C/60 ± 5% RH	Bromelain	100.00 ± 1.23	95.45 ± 2.34	90.46 ± 1.11	85.86 ± 1.90	81.23 ± 2.34	73.12 ± 4.32	8.06×10^{-4}	129.02
	H_4	100.00 ± 2.72	99.09 ± 3.67	98.88 ± 2.05	97.81 ± 1.86	96.81 ± 2.05	95.36 ± 3.84	1.15×10^{-4}	903.16
40 ± 2 °C/75 ± 5% RH	Bromelain	100.00 ± 1.23	89.45 ± 3.90	85.90 ± 2.50	74.18 ± 1.79			1.59×10^{-3}	65.44
	H_4	100.00 ± 2.72	98.26 ± 3.01	98.73 ± 3.99	94.77 ± 5.26			2.76×10^{-4}	376.53

*Values are expressed as mean ± SD, Abbreviations: M = month; K_{calc} = calculated first order degradation rate constant; t_{90} = time to reach 90% of initial drug concentration.

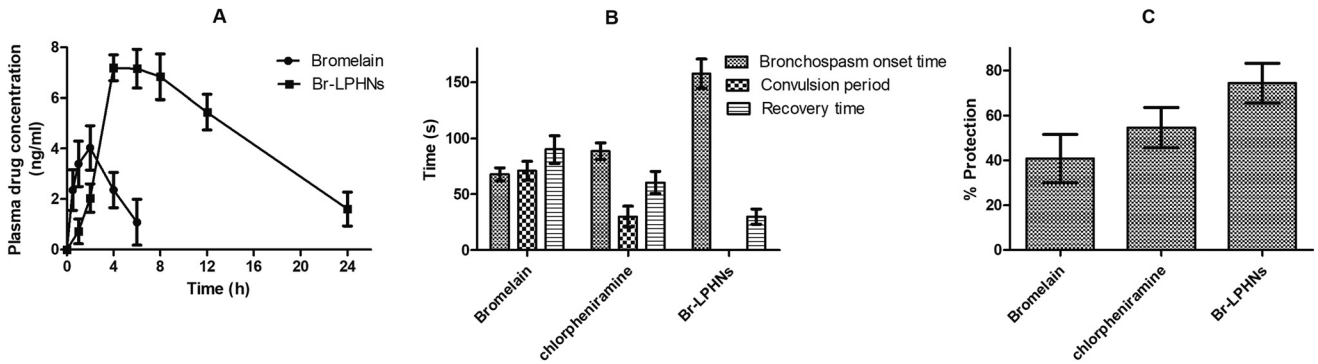

Fig. 3 (A) Plasma drug concentration-time profile of bromelain solution and Br-LPHNs. Effect of bromelain, Br-LPHNs and chlorpheniramine on (B) bronchospasm onset time, recovery time and convulsion period and (C) %protection respectively.

liquefaction, followed by a robust influence on the viscosity of artificial mucus similar to the pure drug after 4 h (Fig. 2). The slow drug release behavior of Br-LPHNs contributed to the lower mucolytic activity of the formulation during the initial hours. However, mucus viscosity significantly reduced with the progression of time due to the deeper penetration of the nanoparticulate formulation into the microarchitecture and mesh spacing of the artificial mucus.[47] In addition, the progressive release of bromelain from Br-LPHNs prevented the end-product inhibition effect observed with pure bromelain and contributed to higher mucolytic activity over a longer duration.[48]

Table 3 Pharmacokinetic parameters of pure drug and optimized formulation obtained after oral administration

Parameter	Pure drug	Formulation
C_{max} (ng ml^{-1})*	4.02 ± 1.09	7.18 ± 2.90
T_{max} (h)*	2.00 ± 0.11	4.00 ± 0.21
K_e (h^{-1})*	0.33 ± 0.11	0.08 ± 0.01
$t_{1/2}$ (h)*	2.11 ± 0.32	7.51 ± 0.51
MRT (h)*	3.18 ± 0.49	10.58 ± 0.93
AUC (ng h^2 ml^{-1})*	15.58 ± 3.22	107.50 ± 13.12
Relative bioavailability (%)		689.99

*$p < 0.05$ level of significant difference.

Stability studies

The effect of storage conditions on the proteolytic activity of pure drug and Br-LPHNs under accelerated and room temperature conditions respectively is presented in Table 2. Pure drug under accelerated and room temperature conditions showed a remarkable decrease in proteolytic activity, expressed as drug content, compared to Br-LPHNs. Bromelain followed first-order degradation kinetics. A lower K_{cal} (calculated degradation rate constant) and higher calculated t_{90} (time to reach 90% of initial concentration) value (~6.99 folds) for the formulation compared to the pure drug indicated significantly better stability of the formulation under real-time stability conditions.[43] Visual changes in the color of the pure drug from off-white to brown were observed at both room and accelerated temperature storage conditions, whereas no color change was observed for Br-LPHNs. This further indicated that the formulation parameters were appropriately optimized to create a stable bromelain-loaded nano-formulation.

Pharmacokinetic studies

The plasma drug concentration-time profiles following oral administration of the free drug and Br-LPHNs in Wistar rats are shown in Fig. 3A. The optimized formulation, after a single-dose administration, showed a significantly ($p < 0.05$) higher C_{max} (1.78-fold) compared to pure bromelain. The increased C_{max} may be contributed to the protection provided by the carrier system

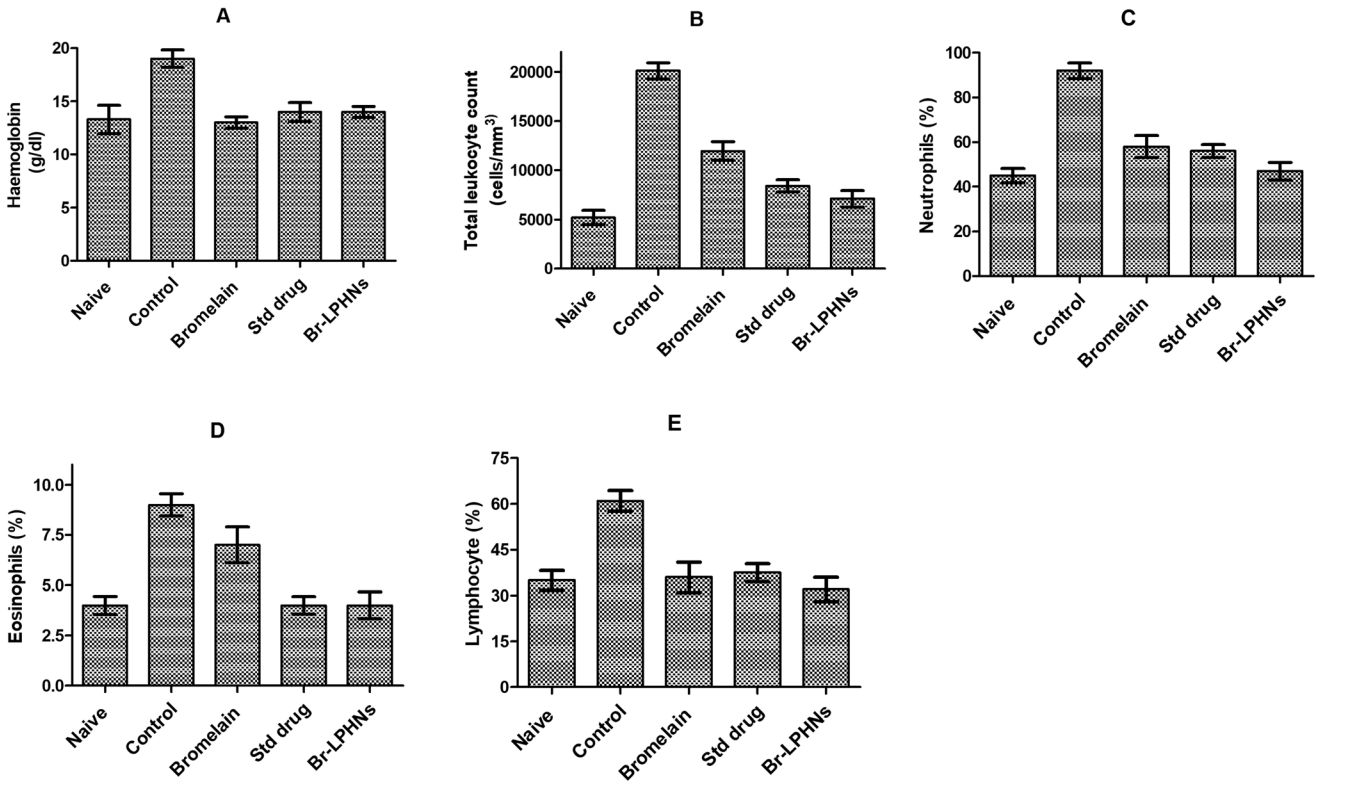

Fig. 4 Hematological biomarker profile of different groups: (A) hemoglobin content, (B) total leucocyte count, (C) neutrophil (%), (D) eosinophil (%) and (E) lymphocyte (%) respectively.

to bromelain in the gastric environment, along with the absorption of nanoparticles *via* specific uptake mechanisms facilitated by their nanoscale size and hydrophobic surface, enhancing permeation across the GIT. The delayed T_{max} (2-fold) also confirmed the sustained *in vivo* bromelain release from the optimized Br-LPHNs formulation, consistent with the *in vitro* drug release study. The shorter $t_{1/2}$ and low systemic mean residence time (MRT) of the pure drug indicated its faster systemic clearance (p

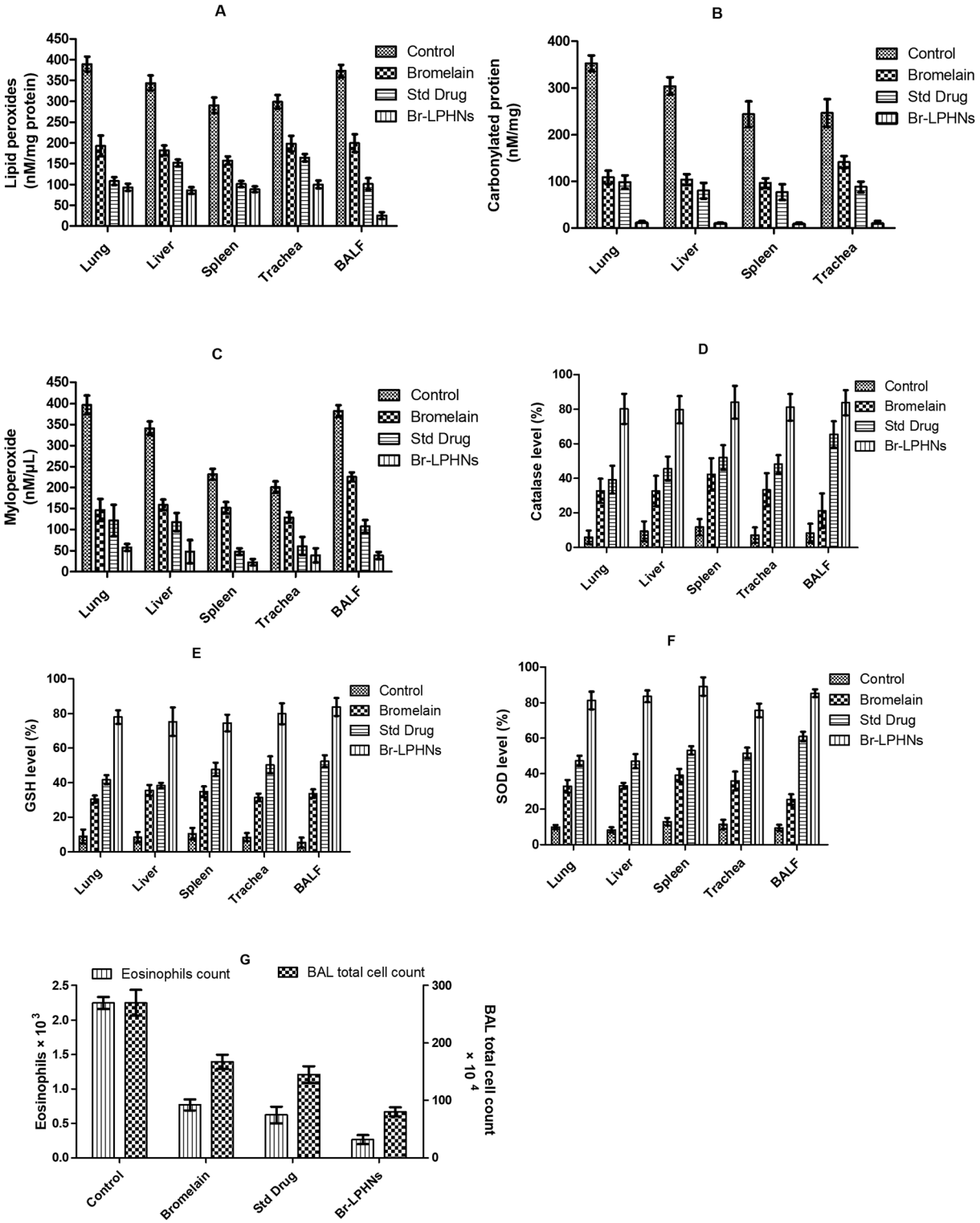

Fig. 5 Effect of different treatments on the levels of (A) LPO, (B) carbonylated protein, (C) MPO, (D) catalase, (E) GSH (F) SOD activity and (G) total cell count and (F) Eosinophil count in bronchoalveolar fluid respectively.

< 0.05). In contrast, Br-LPHNs exhibited higher $t_{1/2}$ (3.38-fold) and MRT (3.32-fold), indicating prolonged systemic absorption and a slower release of the drug into the systemic circulation. Meanwhile, AUC_{0-24h} was also significantly increased, up to 6.89-fold, for the formulation compared to the pure drug (Table 3) ($p < 0.05$). The apparent bromelain loading in LPHNs might have contributed in bypassing extensive gut wall metabolism due to the intimate association of the drug with the lipid–polymeric shell, thereby improving bioavailability. In addition, lymphatic uptake *via* specialized absorption mechanisms such as paracellular and transcellular transport, including endocytosis and M-cells of Payer's patches, might have further enhanced bioavailability.[29,49,50]

Ovalbumin-induced asthma model

In the present study, OVA sensitization induced remarkable airway hyperresponsiveness to histamine challenge.[51] Bronchospasm onsets, recurrent episodes of jerks and recovery time from difficulty in breathing in response to histamine exposure were the major clinical parameters evaluated to determine the efficacy of various treatments (Fig. 3B).[52] Bronchial hyperresponsiveness to histamine in OVA-sensitized animals was significantly higher than in normal saline-sensitized animals ($p < 0.05$). A significant increase in the duration of histamine-induced bronchospasm by 11.14%, 45.08% and 157.37%, and a reduction in recovery time after bronchospasm induction by 48.14%, 64.80% and 82.57% were observed in animals treated with the pure drug, chlorpheniramine and optimized formulation, respectively, compared to control animals ($p < 0.05$). However, Br-LPHNs significantly suppressed bronchial hyperresponsiveness by delaying bronchospasm onset by 292.46%, 120.69% and 67.08% compared to the saline-treated, bromelain-treated and chlorpheniramine-treated groups, respectively. Br-LPHNs offered significantly greater protection against asphyxia than both the pure drug and chlorpheniramine ($p < 0.05$) (Fig. 3C). The greater protective effect of Br-LPHNs might be attributed to the higher systemic bioavailability of bromelain, resulting from the protection offered by the PMMA polymer in the acidic gastric environment and the prolonged drug release characteristic of the optimized formulation.[47] Br-LPHNs effectively counteracted histamine-induced bronchoconstriction, similar to chlorpheniramine, indicating an antihistaminic effect of bromelain.

Hematological evaluation

OVA-sensitized animals showed significant increase in total leukocyte count, eosinophils, lymphocytes, neutrophils and hemoglobin compared to naïve animals (Fig. 4). The elevated

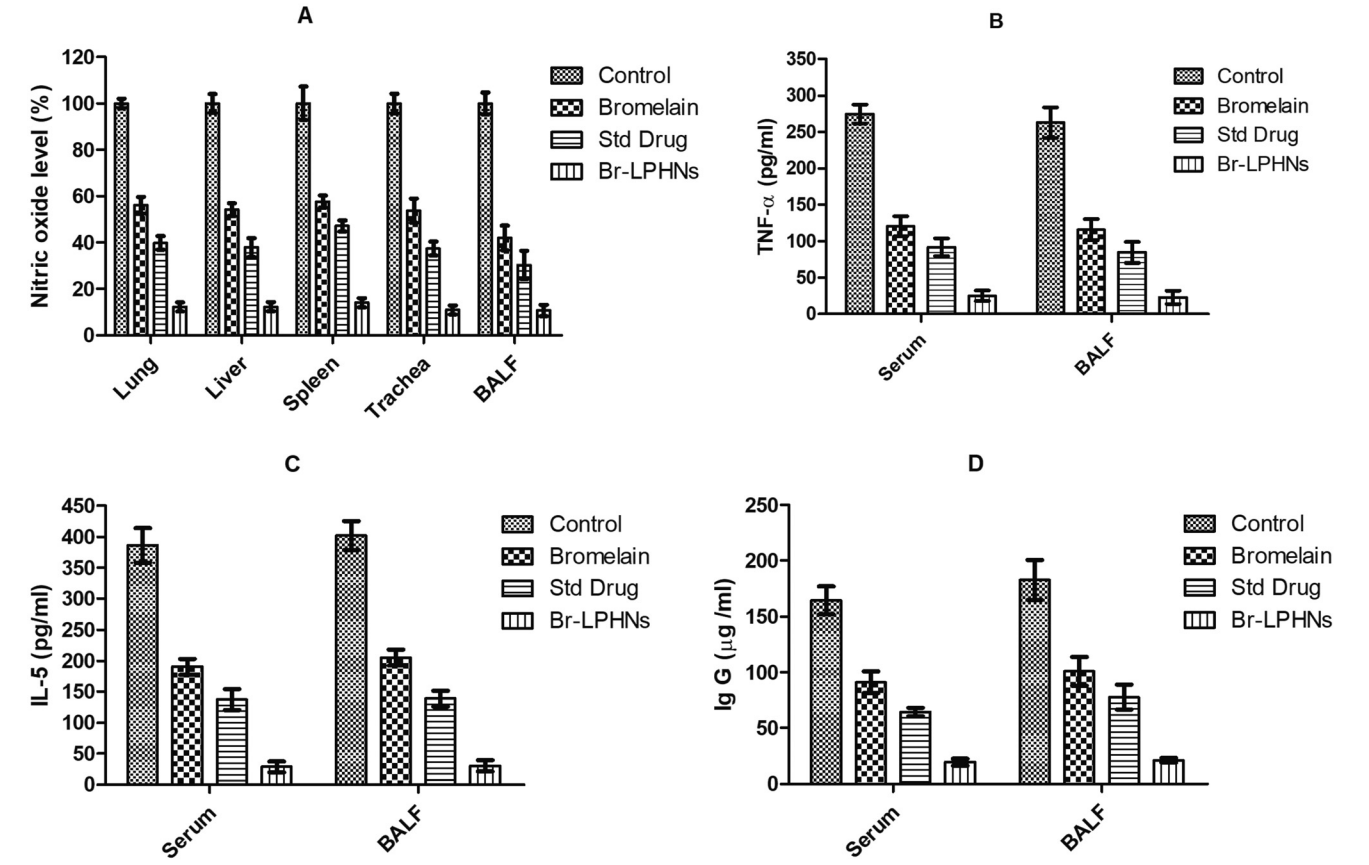

Fig. 6 Assessment of changes in immunological biomarkers: (A) NO in tissue homogenates; (B) TNF-α, (C) IL-5 and (D) Ig-G in serum and BALF in different test group animals.

eosinophil count confirmed the allergic inflammation associated with bronchial hyperresponsiveness.[53] Increased total leukocyte and lymphocyte counts further corroborated the inflammatory state in OVA-sensitized animals. The elevated WBC count induced an unrestricted release of histamine in the lungs of OVA-sensitized animals, leading to symptoms such as runny nose and wheezing during allergen exposure.[54] Oral treatment with Br-LPHNs, compared to the pure drug, significantly ($p < 0.05$) inhibited the progression of allergen-induced asthma by reducing total leukocyte, lymphocyte, neutrophil and eosinophil counts, similar to the chlorpheniramine treatment (Fig. 4). The reversal of hematological markers to levels closer to normal corresponded well with the increased bioavailability of bromelain *via* the carrier system, *i.e.*, Br-LPHNs.

Oxidative and immunological markers

Carbonylated protein, MPO and LPO are key markers of oxidative stress and play a vital role in the pathogenesis of asthma. Under normal physiological conditions, oxidative free radical-induced damage is prevented and resolved by endogenous enzymatic (SOD and CAT) and non-enzymatic (reduced glutathione) defense mechanisms. OVA sensitization induced oxidative cellular stress by disrupting the balance between free radical formation and antioxidant defense, as evidenced by decreased levels of SOD, CAT and GSH, and escalated levels of LPO, MPO and carbonylated protein (Fig. 5).[55] The elevated total cell count (3.47-fold) in BAL fluid too confirmed the infiltration of neutophils and lymphocytes in the lungs, which contributes to lung inflammation, mucus production and edema.

Bromelain, chlorpheniramine and Br-LPHNs displayed notable alleviation of oxidative stress by reducing LPO and carbonylated protein levels in the lung, BALF, liver, trachea and spleen tissues ($p < 0.05$) (Fig. 5). The results demonstrated the effectiveness of Br-LPHNs in suppressing oxidative stress markers and enhancing antioxidant defense compared to pure bromelain and chlorpheniramine ($p < 0.05$) (Fig. 5). The significantly improved antioxidant activity of Br-LPHNs might be ascribed to improved lymphatic uptake *via* phagocytosis and paracellular pathways, along with the preservation of bromelain's activity in the stomach and sustained drug release from the formulation.[14,27]

In the OVA-sensitized control group, the elevated NO level suggested the activation of prostaglandin synthesis and inducible nitric oxide synthase (iNOS) (Fig. 6).[56] Similarly, escalated TNF-α and IL-5 serum levels stipulated the formation of reactive oxygen species, NO synthesis and neutrophil migration to tissues.[57] However, notable depletion of WBC count, MPO, NO, Ig-G, IL-6 and TNF-α levels was observed with Br-LPHNs treatment compared to bromelain (Fig. 6). Thus, it can be inferred that bromelain's favorable antioxidant and anti-inflammatory effects in the treatment of inflammatory disorders like asthma are mediated by its inhibitory influence on NF-κB overexpression and iNOS, as well as the enhanced expression of the Nrf2 pathway.[19,21,58] Br-LPHNs' increased anti-inflammatory efficacy might be attributed to its improved stability in the stomach and prolonged drug release characteristics, which provide long-term inhibitory effect on the cytokine storm.

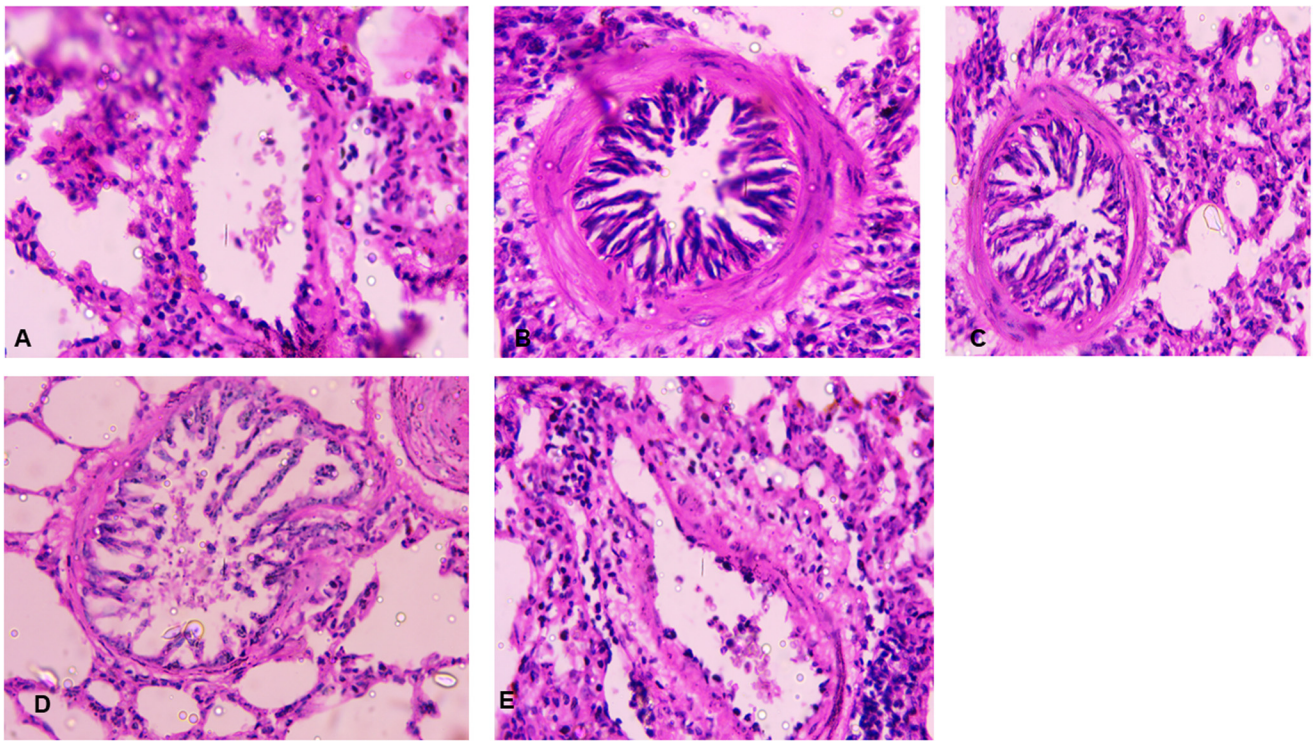

Fig. 7 Microscopic images of lung-sections from saline sensitized guinea pigs (A) naïve and ovalbumin-sensitized (B) saline, (C) bromelain, (D) chlorpheniramine and (E) Br-LPHNs-treated animals respectively.

Histopathological analysis

The lung microphotographs of the naïve group revealed clean alveolar sacs with no cell accumulation in the bronchiole region (Fig. 7A). In contrast, OVA-sensitized lungs showed dense cell infiltration around the bronchioles, blood vessels and alveolar regions, suggesting that excessive cell infiltration led to the constriction of the alveolar sacs (Fig. 7B). Lung tissue remodeling and inflammation may have been caused by oxidative stress induced by the OVA challenge.[55] Less cell aggregation around the bronchioles and reduced thickening of the alveolar septa were observed in the groups treated with bromelain and chlorpheniramine (Fig. 7C and D). However, no thickening around the bronchioles and minimal cell accumulation were observed in the formulation-treated group (Fig. 7E).[5]

Conclusions

Br-LPHNs were successfully fabricated using the double emulsion solvent evaporation method to develop a new therapy for the management of allergic asthma. The hybridization of the lipid core containing the drug with a polymer coat *via* emulsification augmented the drug load, improved bromelain's gastric stability and facilitated prolonged drug release, resulting in higher bioavailability and therapeutic efficacy. Br-LPHNs administration remarkably reduced allergen-induced airway hyperresponsiveness and infiltration of inflammatory cells in lung tissues. The improved anti-inflammatory, antioxidant and anti-asthmatic activities of Br-LPHNs suggested its broader applicability in the treatment of asthma and other disorders associated with oxidative stress and inflammation. However, the scalability of the formulation, along with its efficacy in clinical trials, must be evaluated before the successful implementation of Br-LPHNs in clinical practice.

Author contributions

Manu Sharma: conceptualization, methodology, investigation, supervision, writing – reviewing and editing. Namita Gupta: data curation, investigation, writing – reviewing and editing.

Data availability

The datasets generated during and/or analysed during the current study are available from the corresponding author upon reasonable request.

Conflicts of interest

The authors report no conflicts of interest.

Acknowledgements

The authors acknowledge the Department of Pharmacy, Banasthali Vidyapith (Rajasthan, India), for providing facilities to conduct this research.

References

1 K. R. Ahmadi and D. B. Goldstein, *Curr. Biol.*, 2002, **12**, R702–R704.
2 C. Ober, *Immunol. Rev.*, 2011, **242**, 10–30.
3 A. James and G. Hedlin, *Curr. Treat. Options Allergy*, 2016, **3**, 439–452.
4 I. D. Pavord, R. Beasley, A. Agusti, G. P. Anderson, E. Bel, G. Brusselle, P. Cullinan, A. Custovic, F. M. Ducharme, J. V. Fahy, U. Frey, P. Gibson, L. G. Heaney, P. G. Holt, M. Humbert, C. M. Lloyd, G. Marks, F. D. Martinez, P. D. Sly and A. Bush, *Lancet*, 2018, **391**, 350–400.
5 M. Tiwari, U. N. Dwivedi and P. Kakkar, *J. Ethnopharmacol.*, 2014, **153**, 326–337.
6 L. M. Graham, *J. Allergy Clin. Immunol.*, 2002, **109**, 560–566.
7 R. Dahl, *Respir. Med.*, 2006, **100**, 1307–1317.
8 H. M. El-Laithy, A. Youssef, S. S. El-Husseney, N. S. El Sayed and A. Maher, *Drug Delivery*, 2021, **28**, 826–843.
9 F. Carmona and A. S. Pereira, *Rev. Bras. Farmacogn.*, 2013, **23**, 379–385.
10 A. J. Chakraborty, S. Mitra, T. E. Tallei, A. M. Tareq, F. Nainu, D. Cicia, K. Dhama, T. Emran, J. Simal-Gandara and R. Capasso, *Life*, 2021, **11**, 1–26.
11 A. R. Lam, K. Bazzi, S. J. Valle and D. L. Morris, *Case Rep. Oncol.*, 2021, **14**, 628–633.
12 S. Soheilifar, M. Bidgoli, A. Hooshyarfard, A. Shahbazi, F. Vahdatinia and F. Khoshkhooie, *J. Dent.*, 2018, **15**, 309–316.
13 M. Azarkan, M. M. González, R. C. Esposito and M. E. Errasti, *Protein Pept. Lett.*, 2020, **27**, 1159–1170.
14 M. Sharma and D. Chaudhary, *Nanomedicine*, 2022, **22**, 102543.
15 M. Sharma and R. Sharma, *RSC Adv.*, 2018, **8**, 2541–2551.
16 M. Sharma and D. Chaudhary, *Int. J. Pharm.*, 2021, **594**, 120176.
17 T. C. Chang, P. L. Wei, P. T. Makondi, W. T. Chen, C. Y. Huang and Y. J. Chang, *PLoS One*, 2019, **14**, e0210274.
18 S. Müller, R. März, M. Schmolz, B. Drewelow, K. Eschmann and P. Meiser, *Phytother. Res.*, 2013, **27**, 199–204.
19 J. R. Huang, C. C. Wu, R. C. Hou and K. C. Jeng, *Immunol. Invest.*, 2008, **37**, 263–277.
20 E. R. Secor, W. F. Carson, A. Singh, M. Pensa, L. A. Guernsey, C. M. Schramm and R. S. Thrall, *J. Evidence-Based Complementary Altern. Med.*, 2008, **5**, 61–69.
21 K. Bhui, S. Prasad, J. George and Y. Shukla, *Cancer Lett.*, 2009, **282**, 167–176.
22 L. P. Hale, P. K. Greer, C. T. Trinh and M. R. Gottfried, *Clin. Immunol.*, 2005, **116**, 135–142.

23 L. Desser, D. Holomanova, E. Zavadova, K. Pavelka, T. Mohr and I. Herbacek, *Chemother. Pharmacol.*, 2001, **47**, 10–15.
24 H. Ikushima and K. Miyazono, *Nat. Rev. Cancer*, 2010, **10**, 415–424.
25 L. P. Hale, *Int. Immunopharmacol.*, 2004, **4**, 255–264.
26 N. N. M. Rao, S. Sharma, P. Kaduba, V. Sadhu, M. Sharma and A. V. S. Sainath, *J. Appl. Polym. Sci.*, 2020, **137**, 48954.
27 M. Sharma, S. Sharma and J. Wadhawa, *Artif. Cells, Nanomed., Biotechnol.*, 2019, **47**, 45–55.
28 L. Sercombe, T. Veerati, F. Moheimani, S. Y. Wu, A. K. Sood and S. Hua, *Front. Pharmacol.*, 2015, **6**, 286.
29 R. R. Patel, G. Khan, S. Chaurasia, N. Kumar and B. Mishra, *RSC Adv.*, 2015, **5**, 76491–76506.
30 S. Shah, P. Famta, P. S. Raghuvanshi, S. B. Singh and S. Srivastava, *Colloids Interface Sci. Commun.*, 2022, **46**, 100570.
31 A. Bettencourt and A. J. Almeida, *J. Microencapsulation*, 2012, **29**, 353–367.
32 O. H. Lowry, N. J. Rosebrough, A. L. Farr and R. J. Randall, *J. Biol. Chem.*, 1951, **193**, 265–275.
33 X. Li, Z. Yang and Y. Bai, *Int. J. Biol. Macromol.*, 2018, **10**, 144–156.
34 M. D. A. Hasan, C. F. Lange and M. L. King, *J. Non-Newtonian Fluid Mech.*, 2010, **165**, 1431–1441.
35 A. P. Lowe, K. J. Broadley, A. T. Nials, W. R. Ford and E. J. Kidd, *J. Pharmacol. Toxicol. Methods*, 2015, **72**, 85–93.
36 G. A. Koffuor, A. Boye, S. Kyei, J. Ofori-Amoah, E. A. Asiamah, A. Barku, J. Acheampong, E. Amegashie and A. K. Awuku, *Pharm. Biol.*, 2016, **54**, 1354–1363.
37 R. Pichot, R. L. Watson and I. T. Norton, *Int. J. Mol. Sci.*, 2013, **14**, 11767–11794.
38 M. A. Schubert and C. C. Müller-Goymann, *Eur. J. Pharm. Biopharm.*, 2005, **61**, 77–86.
39 L. Zhang, J. M. Chan, F. X. Gu, J. W. Rhee, A. Z. Wang, A. F. Radovic-Moreno, F. Alexis, R. Langer and O. C. Farokhzad, *ACS Nano*, 2008, **2**, 1696–1702.
40 M. Sharma, V. Sharma, A. K. Panda and D. K. Majumdar, *Pharm. Dev. Technol.*, 2013, **18**, 560–569.
41 A. B. T. Ghisaidoobe and S. J. Chung, *Int. J. Mol. Sci.*, 2014, **15**, 22518–22538.
42 S. K. Haq, S. Rasheedi and R. H. Khan, *Eur. J. Biochem.*, 2002, **269**, 47–52.
43 M. Sharma, V. Sharma, A. K. Panda and D. K. Majumdar, *Int. J. Nanomed.*, 2011, **6**, 2097–2111.
44 H. L. Jian, X. J. Lin, W. A. Zhang, W. M. Zhang, D. F. Sun and J. X. Jiang, *Food Hydrocolloids*, 2014, **40**, 115–121.
45 K. Pillai, J. Akhter, T. C. Chua and D. L. Morris, *Int. J. Cancer Res.*, 2014, **134**, 478–486.
46 S. L. Wang, H. T. Lin, T. W. Liang, Y. J. Chen, Y. H. Yen and S. P. Guo, *Bioresour. Technol.*, 2008, **99**, 4386–4393.
47 C. Müller, K. Leithner, S. Hauptstein, F. Hintzen, W. Salvenmoser and A. Bernkop-Schnürch, *J. Nanopart. Res.*, 2013, **15**, 1–13.
48 M. Sharma, V. Sharma and D. K. Majumdar, *Int. Scholarly Res. Not.*, 2014, **2014**, 1–8.
49 W. Wang, R. Zhu, Q. Xie, A. Li, Y. Xiao, K. Li, H. Liu, D. Cui, Y. Chen and S. Wang, *Int. J. Nanomedicine*, 2012, **7**, 3667–3677.
50 G. Sahay, D. Y. Alakhova and A. V. Kabanov, *J. Controlled Release*, 2010, **145**, 182–195.
51 V. Zugic, N. Mujovic, S. Hromis, J. Jankovic, M. Drvenica, A. Perovic, I. Kopitovic, A. Ilic and D. Nikolic, *J. Clin. Med.*, 2018, **7**, 1–9.
52 P. J. Mauser, A. House, H. Jones, C. Correll, C. Boyce and R. D. Chapman, *Pulm. Pharmacol. Ther.*, 2013, **26**, 677–684.
53 K. Nakagome and M. Nagata, *Front. Immunol.*, 2018, **9**, 2220.
54 T. Hailemaryam, W. Adissu, L. Gedefaw and Y. Asres, *Hematol. Transfus. Int. J.*, 2018, **6**, 77–82.
55 A. O. Antwi, D. D. Obiri and N. Osafo, *Mediators Inflammation*, 2017, 1–11.
56 A. Hori, M. Fujimura, N. Ohkura and A. Tokuda, *Cough*, 2011, **7**, 5.
57 Z. Cai, J. Liu, H. Bian and J. Cai, *Am. J. Transl. Res.*, 2019, **11**, 7300–7309.
58 K. Bhui, S. Tyagi, A. K. Srivastava, M. Singh, P. Roy, R. Singh and Y. Shukla, *Mol. Carcinog.*, 2012, **51**, 231–243.